UKACC International Conference on Control 2012
Cardiff, UK, 3-5 September 2012

System Identification and Robust Anti-windup Control for a Helium Liquifier

Jing Na, Guang Li, Ryuji Maekawa and Luigi Serio

Abstract— **This paper addresses the system identification and advanced control of a helium (He) liquifier supplying cooling power at liquid helium (LHe) temperatures (-269 $^{\circ}$C). To study the dynamic response to heat load variation, a He liquifier simulation model is utilized. The main focus is to regulate the discharge pressure of the compressor station to guarantee stable system operation. System identification is first conducted to obtain plant models, and a two degree of freedom H_∞ controller is designed to achieve regulation. Moreover, saturation of the control valve is compensated via an anti-windup technique, which is suitable for regulation problem with disturbance rejection. The effectiveness of the proposed control designs is demonstrated by dynamical simulations in EcosimPro (*EA International*) software.**

Index Terms— **Helium liquefier, anti-windup, robust control, disturbance rejection.**

I. Introduction

ITER [1] that is now under construction at Cadarache, South of France is designed to demonstrate the scientific and technical feasibility of nuclear fusion as a primary source of virtually inexhaustible energy. It is the biggest fusion energy research project, and one of the most challenging and innovative scientific endeavors in the world today [2]. The machine requires high magnetic fields to confine and stabilize the plasma. For such a facility, a cryogenic system will be employed to cool-down and maintain the superconductivity state of the magnets. The ITER cryogenic system [3], [4] will be one of the largest cryogenic systems in the world with a refrigeration capacity of 65 kW equivalent at 4.5 Kelvin.

In cryogenic systems, various components (e.g. heat exchangers, valves, turbines, compressors, etc.) are employed, and the associated controllers are required. To facilitate the control design, several dynamic simulators have been developed, e.g. C-PREST for LHD [5], PROCOS for LHC [6], [7]. Based on dynamic simulators, some advanced control methods have also been presented, for example, internal model control (IMC) [8], nonlinear model predictive control (MPC) [9] and other methods [10], [11]. In these schemes, the discharge pressure of the compressor station (CS) is regulated to guarantee the stable system operation. In [8] and [10], system identification method is also utilized. However, the modeling uncertainties are not explicitly considered in the control design and the potential control valve saturation is not studied.

To address the aforementioned issues, this paper proposes an alternative system identification and advanced control design method. A helium liquefier simulation model originally designed in [12] is employed as the plant to be controlled. However, to facilitate the control design, modifications on the CS control configuration have been done (will be explained in Section II). Moreover, to study the dynamic response of the liquefier, time-varying heat loads are applied in the reservoir. The major focus of this study is to regulate the discharge pressure of CS under dynamic heat loads to sustain the system stability.

The frequency-domain system identification is conducted to obtain the mathematical models, which are supposed to cover system dynamics in a wide frequency band compared to those models from the time-domain identification. Then a H_∞ robust controller [13], [14] is designed to accommodate the modeling uncertainties. Moreover, to recover the control performance in the presence of the control valve saturation, a robust disturbance rejection anti-windup framework (DRAW) recently developed in [15] is employed. The salient feature is that the modeling uncertainties and the disturbance rejection can be incorporated into the AW compensator design and synthesis. Simulation results in a commercial software, EcosimPro [16], are provided to illustrate the performance improvement over alternative approaches. Hence the main contribution of this paper is to provide a systematic robust anti-windup control design procedure for CS pressure regulation of He liquifier with dynamic heat loads, based on frequency system identification and advanced control strategies.

II. Helium liquifier

Commercial modeling and simulation software, EcosimPro [16], has recently been used for cryogenic simulations. With this software, a cyo-library has been developed by researchers [6], [7], [8] at the European Organization for Nuclear Research (CERN). In this library, various cryogenic component models are constructed based on the mass flowrate and energy balance and the helium properties are obtained from the helium library HEPAK [17].

A. Helium liquefier model

A helium liquefier designed by CERN [12] is adopted in this study. The liquefier consists of a warm compressor station (CS) and a cold-box (CB) including two expansion turbines (TU), four heat exchangers (HX), a LHe reservoir and connecting pipes and valves. The overall process and instrument diagram (P &ID) is depicted in Fig.1. The CS model and CB model and their associated control structure simulated in EcosimPro are shown in Fig.2 and Fig.3. The entire model contains 1799 differential and algebraic equations (DAEs) with 157 derivatives, 21 boundary variables and 10 control loops.

J. Na, R. Maekawa and L. Serio are with ITER Organization, Route de Vinon sur Verdon, 13115 Saint Paul Lez Durance, France. {Jing.Na, Ryuji.Maekawa,Luigi.Serio}@iter.org

G. Li is with School of Engineering, Computing and Mathematics, University of Exeter, Harrison Building, Streatham Campus, North Park Road, Exeter, EX4 4QF, UK. g.li@exeter.ac.uk

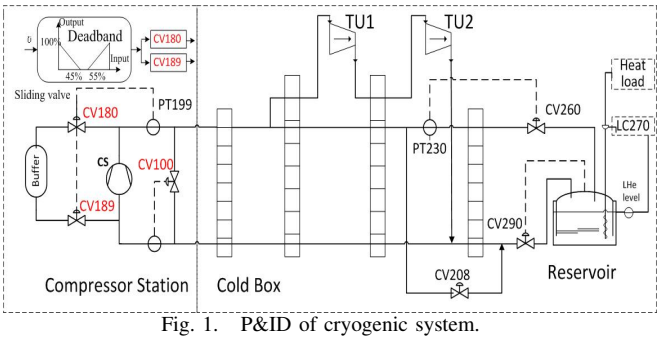

Fig. 1. P&ID of cryogenic system.

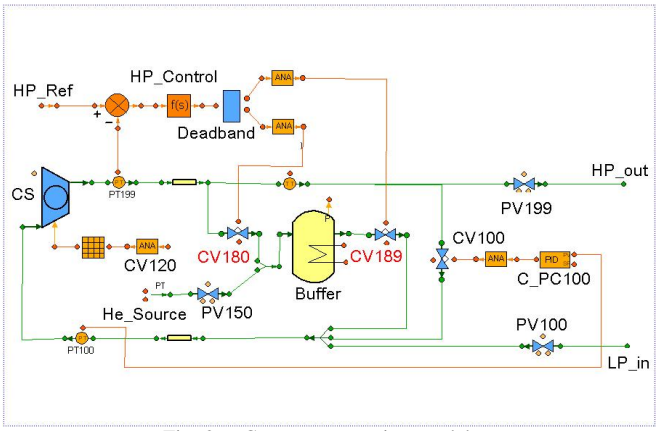

Fig. 2. Compressor station model.

The compressor station compresses helium from 0.1 MPa to 1.3 MPa providing mass flowrate 100 g/s. The discharge pressure or high pressure (HP) is regulated by two antagonist valves: the discharge valve (CV180) that removes the high pressure He into the buffer and a charge valve (CV189) that charges the low pressure from the buffer. It should be pointed out that in the original model proposed in [12], two separated PI controllers with different setpoints are utilized for valves CV180 and CV189. However, in this study the control configuration of CV180 and CV189 is modified to reduce the complexity of control design and to improve the performance. As shown in the left top of Fig.1, the HP is regulated by controlling a split-range valve with a deadband between MV=45%-55%, where the deadband takes the controller output as the input and the corresponding stem positions of the discharge valve CV180 and charge valve CV189 as the outputs. In this case, only one controller (i.e. HP_Control in Fig.2) is required for operating the valves CV180 and CV189 simultaneously. Moreover, the low pressure (LP) is regulated by a bypass valve CV100 connecting HP and LP.

In the cold-box (Fig.3), the inlet valves of turbines (TU1, TU2) are controlled based on their input pressures and the output temperatures. The Joule-Thomson (J-T) valve is controlled taking the inlet pressure as the control variable. The LHe level in the reservoir is regulated by means of an embedded electrical heater with a PI control.

B. Control problem formulation

To simulate the dynamic response of the liquifier (as shown in Fig.1), the time-varying heat loads are directly applied in the reservoir [10]. In this case, the pressure

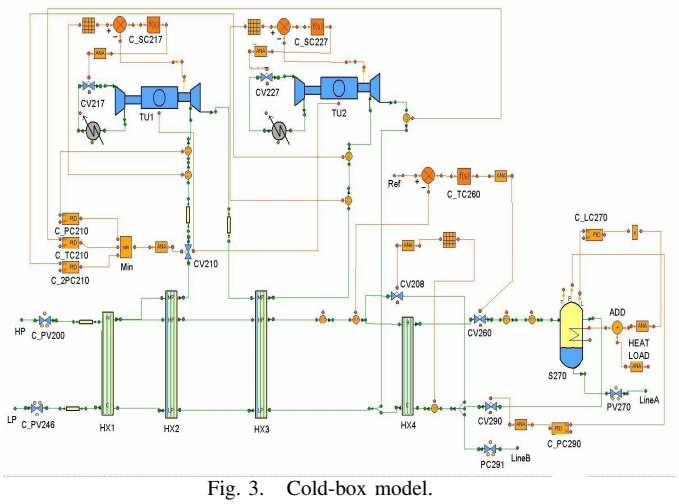

Fig. 3. Cold-box model.

fluctuations caused by the LHe evaporation (due to the heat loads) may deteriorate the system stability or even trigger instability (e.g. turbine trips) in the worst case. To sustain system stability and the LHe product, as explained in [11], several conditions should be guaranteed: 1) the HP and LP need to be regulated at the *a prior* designed constants (or within fixed intervals) to ensure the reliability of compressor; 2) the LHe level in the reservoir has to stay within an acceptable level to avoid drying or overflow.

To fulfil the requirement 1), we propose an alternative control design strategy for the liquifier (Fig.1) to regulate the HP of CS under dynamic heat loads. In particular, the control valve saturation is considered via an anit-windup (AW) compensator. Other control loops in the cold box are operated with PI controls guaranteeing also condition 2).

III. Plant Model Identification

As shown in Fig.1, the HP regulation can be achieved by controlling the sliding valve (CV180/CV189). The heat load applied in the LHe reservoir is taken as the disturbance $d(t)$, the HP of CS is taken as the output $y(t)$, and the position of sliding valve (CV180/CV189) is taken as the input $u(t)$ which is constrained within $[0,100]$ (i.e. valves should be opened between 0% - 100%). Then the overall system dynamics can be described as

$$Y(s) = G_u(s)U(s) + G_d(s)D(s) \tag{1}$$

where $Y(s), U(s)$ and $D(s)$ are the Laplace transform of $y(t), u(t)$ and $d(t)$, respectively. The transfer function G_u denotes the dynamics from the control input u to output y and G_d denotes the dynamics from the disturbance d to output y.

Note there are some nonlinearities (e.g. deadband) in the system (Fig.1). For ease of system identification and control design, linear transfer function (1) is used to represent the main system dynamics and the modeling uncertainties will be considered in the control design in terms of robust control scheme. To obtain models $G_u(s)$ and $G_d(s)$ under wide operation conditions, a frequency identification method based on the correction analysis [18] is adopted. The identification procedure is briefly summarized as follows:

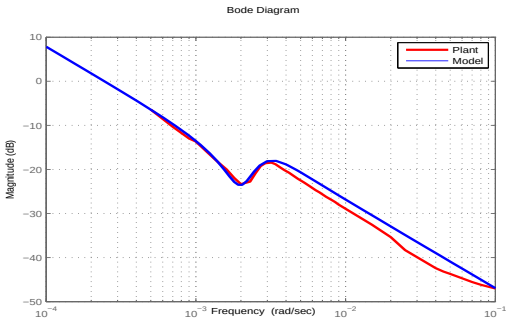

Fig. 4. Process model $G_u(s)$ (2) validation.

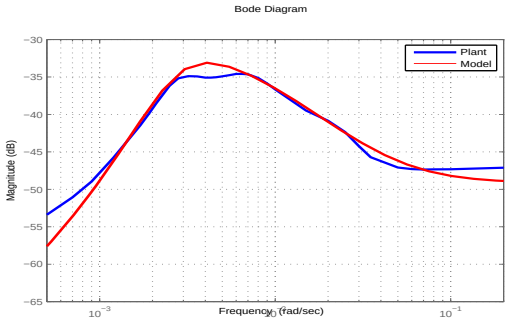

Fig. 5. Disturbance model $G_d(s)$ (3) validation.

1) Apply sinusoidal signals $u(t) = a_1 + b_1 sin(\omega t)$ as the system input and/or $d(t) = a_2 + b_2 sin(\omega t)$ as the disturbance with $a_i > 0, b_i > 0$, and then record the output $y(t)$;

2) Conduct the correlation analysis for data set $(u(t), y(t)), t \in [0, T]$ to deduce the auto-correlation functions $R_u(\omega)$, $R_d(\omega)$, $R_y(\omega)$ and cross-correlation functions $R_{uy}(\omega)$, $R_{dy}(\omega)$. Then calculate the magnitude $H_u(\omega)$, $H_d(\omega)$ and phase $\phi_u(\omega)$, $\phi_d(\omega)$ corresponding to frequency ω by using $R_u(\omega)$, $R_d(\omega)$, $R_y(\omega)$ and $R_{uy}(\omega)$, $R_{dy}(\omega)$.

3) Change the frequency ω, and repeat calculations 2) for a number of frequencies in the studied frequency band.

4) Plot the magnitude and phase responses $\phi_i(\omega), H_i(\omega), i = u, d$ versus frequency ω.

5) Derive the mathematical models from the plotted Bode diagrams via the curve fitting method.

In this study, the signal $u(t) = 51 + 10 sin(\omega t)$ with ω=0.0005∼0.8 rad/s is used as the input and $d(t) = 200 + 80 sin(\omega t)$ Watt with ω=0.0001∼0.3 rad/s is employed as the disturbance. 45 group of data sets for $(u(t), y(t))$ and 37 group of data sets for $(d(t), y(t))$ are recorded. Then following the above identification steps, we can derive the process model as

$$G_u(s) = K_u \frac{(s^2 + 2\xi_1 \omega_{n1} s + \omega_{n1}^2)}{s(s^2 + 2\xi_2 \omega_{n2} s + \omega_{n2}^2)} \tag{2}$$

with $\xi_1 = 0.2$, $\omega_{n1} = 0.002$, $\xi_2 = 0.4$, $\omega_{n2} = 0.0027$, $K_u = 4.5 \times 10^{-4}$, and the disturbance model as

$$G_d(s) = K_d \frac{s(1 + \frac{1}{T_1 s})(1 + \frac{1}{T_2 s})}{(s^2 + 2\xi \omega_n s + \omega_n^2)(1 + \frac{1}{1+T_3 s})} \tag{3}$$

with $K_d = 1.995 \times 10^{-5}$, $T_1 = 0.0008$,$T_2 = 0.05$, $T_3 = 0.007$, $\xi = 0.6$, $\omega_n = 0.003$.

For comparison, Fig.4 and Fig.5 provide the magnitude responses versus frequency of process model (2) and disturbance model (3). It is shown that the derived models can capture main dynamics of the liquifier among the studied frequency band, which illustrates the validity of the proposed identification results.

IV. H_∞ CONTROL AND ANTI-WINDUP COMPENSATION

In practice, there are usually unavoidable modeling uncertainties based on process model (2) and disturbance model (3) (as shown in Fig. 4 and Fig. 5). To accommodate unmodeled dynamics, H_∞ synthesis method [13], [14] is used to design a 2-degree-of-freedom (DOF) controller $K(s)$. Moreover, since the sliding valve (CV180/CV189) can only be opened between 0-100%, an anti-windup compensator [15] is further incorporated to compensate for the valve saturation.

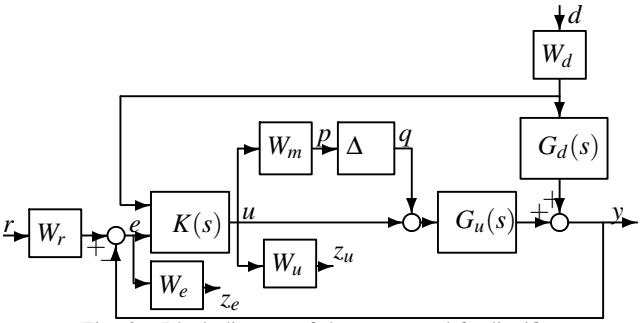

Fig. 6. Block diagram of the H_∞ control for liquifier

A. H_∞ controller design

The scheme for H_∞ controller design of the liquifier is illustrated in Fig. 6. In this case, the plant model is supposed to be an input-multiplicative uncertainty model

$$\tilde{G}_u(s) = G_u(s)(1 + W_m(s)\Delta(s)), \tag{4}$$

where the uncertainty $\|\Delta(s)\|_\infty \leq 1$ and $W_m(s)$ is a weighting function. This uncertainty represents unmodeled dynamics from the control input to output (e.g. difference between the blue line and red line in Fig. 4). The uncertainties from the disturbance to output is not considered in H_∞ controller design, since this uncertainty does not influence the robust stability of the feedback control system. A 2-DOF controller $K(s) = [K_d(s), K_e(s)]$ is designed, where $K_d(s)$ is the feedforward controller and $K_e(s)$ is the feedback controller. The controller $K(s)$ aims to minimize the mapping from $w = [d, r]^T$ to $z = [z_e, z_u]$, represented by $\mathscr{T}_{zw}$. In Fig. 6, the following relations hold

$$\begin{aligned} y &= G_u q + G_d W_d d + G_u u, \\ u &= K_d d + K_e e, \qquad & e &= W_r r - y, \\ z_e &= W_e e, & z_u &= W_u u, \\ p &= W_m u, & q &= \Delta p. \end{aligned}$$

From the above relations, we can derive the following equation for H_∞ control synthesis

$$\begin{bmatrix} p \\ \hline z_e \\ z_u \\ \hline d \\ e \end{bmatrix} = \begin{bmatrix} 0 & 0 & 0 & W_m \\ -W_e G_u & -W_e G_d W_d & W_e W_r & -W_e G_u \\ 0 & 0 & 0 & W_u \\ 0 & W_d & 0 & 0 \\ -G_u & -G_d W_d & W_r & -G_u \end{bmatrix} \begin{bmatrix} q \\ \hline d \\ r \\ \hline u \end{bmatrix} \tag{5}$$

Here the uncertainty weighting function is chosen as $W_m = \frac{2s+0.05}{s+1}$, which represents an increase of unmodelled uncertainties from 5% at low frequency to 200% above 1 rad/s. The tracking performance weighting function is $W_e = \frac{0.25(s+0.4)}{s+2\times10^{-5}}$. The input weighting function is $W_u = \frac{20(s+0.025)}{s+1}$; the magnitude of the weight increases above 0.025 rad/s to limit the closed-loop bandwidth. Those weighting functions should be chosen as a tradeoff between the tracking performance and input magnitude. The disturbance weighting function is chosen as $W_d = \frac{s+1}{s+0.005}$ to describe the high amplitude of the disturbance below 0.005 rad/s. The reference weighting function is $W_r = 1$. Using these weighting functions, an H_∞ controller is synthesized using the commercial routine `hinfsyn` in robust control toolbox of MATLAB®.

B. Anti-windup (AW) compensator design

In order to recover the performance during the control valve saturation (due to the valve hardware constraints), a separate AW compensator is needed [19], [20]. The AW compensator only provides compensation for the control signal when saturation occurs. In this paper, the AW approach recently proposed in [15] is adopted, which can explicitly incorporate the plant uncertainties and disturbance rejection into synthesis, and thus can make a tradeoff between the robustness and performance. The AW approach proposed in [15] is based on the framework shown in Fig. 7. It is assumed that the model has an additive uncertainty Δ_a which is related to (4) by

$$W_a = G_u W_m \tag{6}$$

The plant is $G = [G_d, G_u + W_a\Delta]$ and the controller K is the H_∞ controller designed in the last section. Suppose the right co-prime factorization of $G_u(s)$ is $N(s)M^{-1}(s)$, then the AW compensator takes the form of

$$\begin{bmatrix} M(s)E-I \\ N(s) \end{bmatrix} \sim \left[\begin{array}{c|c} A_p+B_pF & B_pE \\ \hline F & E-I \\ C_p+D_pF & D_pE \end{array}\right] \tag{7}$$

Here $G_u \sim (A_p, B_p, C_p, D_p)$ with $A_p \in \mathbb{R}^{n_p\times n_p}$. $F \in \mathbb{R}^{1\times n_p}$ and $E \in \mathbb{R}$ are the variables to be designed by the AW synthesis approach. The input of the AW compensator is the difference between the input and output signals of the saturation operator, and the AW compensator provides two compensation signals, which are added to the input and output signals of the feedback controller. The essential concept of this AW approach to minimize the $\mathscr{L}_2$ gain of

$$\frac{1}{\gamma_d}\left\| \begin{matrix} W_y^{\frac{1}{2}} y_d \\ W_r^{\frac{1}{2}} u \end{matrix} \right\|^2 - \gamma_d \|d\|^2 \le 0 \tag{8}$$

while incorporating the saturation nonlinearity into synthesis. In (8), the $\mathscr{L}_2$ gains of the mapping from the disturbance d to y_d and the mapping from d to u should be minimized simultaneously. The mapping from d to y_d reflects the performance: a smaller y_d can bring a better performance; the mapping from d to u reflects the robustness: a smaller u leads to a larger margin for robustness. W_y and W_r are weighting matrices, which are positive diagonal and used to tradeoff the gains of the two mappings.

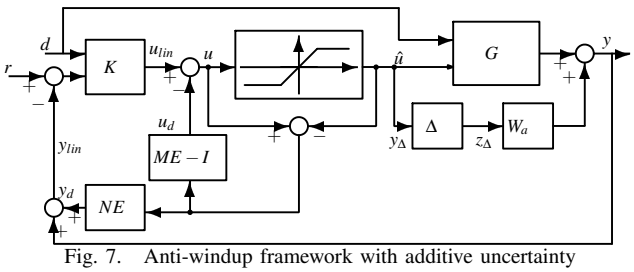

Fig. 7. Anti-windup framework with additive uncertainty

For completeness, the main steps for this AW compensation synthesis procedure is presented (see [15] for more theoretical background and [21] for a real application case.)

1) Compute a disturbance filter

$$P_d := (I - K_y G_u)^{-1}([K_d, w_d] + K_e[G_d, 0])$$

whose state space realization is (A_d, B_d, C_d, D_d) with $A_d \in \mathbb{R}^{n_d\times n_d}$.

2) Given the matrix variable $P = P^T > 0$, solve $\gamma_d^* := \min \gamma_d > 0$ subject to LMI-1 in (9) and LMI-2 in (10) to yield P^* and γ_d^*.

$$\mathbf{LMI-1}: \quad \begin{bmatrix} PA_o + A_o^T P + PW_A + W_A^T P & W_C + PW_B \\ W_C^T + W_B^T P & W_D \end{bmatrix} < 0 \tag{9}$$

with

$$A_o = \begin{bmatrix} A_p & 0 \\ 0 & A_d \end{bmatrix} \qquad W_A = \begin{bmatrix} 0 & B_p C_d \\ 0 & 0 \end{bmatrix}$$

$$W_B = \begin{bmatrix} B_p D_d & 0 & -B_p \\ B_d & 0 & 0 \end{bmatrix} \qquad W_C = \begin{bmatrix} 0 & C_p^T & 0 \\ 0 & C_d^T D_p^T & 0 \end{bmatrix}$$

$$W_D = \begin{bmatrix} -\gamma_d I_{n_w} & D_d^T D_p^T & 0 \\ D_p D_d & -\gamma_d I_{n_y} W_y^{-1} & -D_p \\ 0 & -D_p^T & -\Gamma \end{bmatrix}$$

and

$$\mathbf{LMI-2}: \quad \begin{bmatrix} A_d^T P_{22} + P_{22} A_d & P_{22} B_d & C_d^T \\ B_d^T P_{22} & -\gamma_d I_{n_w} & D_d^T \\ C_d & D_d & -\gamma_d W_r^{-1} \end{bmatrix} < 0 \tag{10}$$

Here the variables are the scalar $\gamma_d > 0$, diagonal matrix $\Gamma = \mathrm{diag}(\gamma_1, \ldots, \gamma_{n_u}) > 0$, and P is a symmetric positive definite matrix with a structure

$$P := \begin{bmatrix} P_{11} & P_{12} \\ P_{12}^T & P_{22} \end{bmatrix} \in \mathbb{R}^{n_p+n_d} \tag{11}$$

3) Substituting P^* and γ_d^* with some chosen diagonal positive definite W, solve the LMI:

$$\Psi + H^T \Lambda G + G^T \Lambda^T H < 0 \tag{12}$$

for Λ, with $\Lambda := \begin{bmatrix} F & E \end{bmatrix}$ and

$$\Psi = \begin{bmatrix} A_o^T P + PA_o & PB_o + C_{do}^T \tilde{W} & C_{po}^T \\ B_o^T P + \tilde{W} C_{do} & \tilde{W} D_{do} + D_{do}^T \tilde{W} - \gamma_d \tilde{I}_{n_w} & 0 \\ C_{po} & 0 & -\gamma_d I_{n_y} \end{bmatrix},$$

$$H = \left[\begin{array}{cc|c|cc} B_p^T & 0 & -1 & 0 & D_p^T \end{array}\right] \mathrm{diag}(P, \tilde{W}, I),$$

$$G = \left[\begin{array}{cc|cc|c} I_{n_p} & 0 & 0 & 0_{n_p\times 1} & 0 \\ 0 & 0 & 1 & 0 & 0 \end{array}\right],$$

where $\tilde{W} = \begin{bmatrix} W & 0 \\ 0 & 1 \end{bmatrix}$, and

$$B_o = \begin{bmatrix} 0_{n_p\times 1} & 0_{n_p\times 1} \\ 0_{n_d\times 1} & B_d \end{bmatrix} \qquad C_{do} = \begin{bmatrix} 0_{1\times n_p} & C_d \\ 0_{1\times n_p} & 0 \end{bmatrix}$$

$$D_{do} = \begin{bmatrix} 0 & D_d \\ 0 & 0 \end{bmatrix} \qquad C_{po} = \begin{bmatrix} C_p & 0 \end{bmatrix}$$

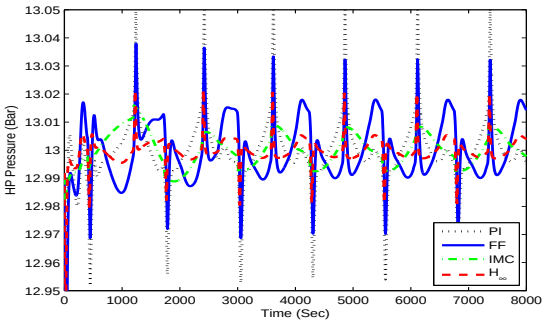

Fig. 8. HP regulation steady-sate performance.

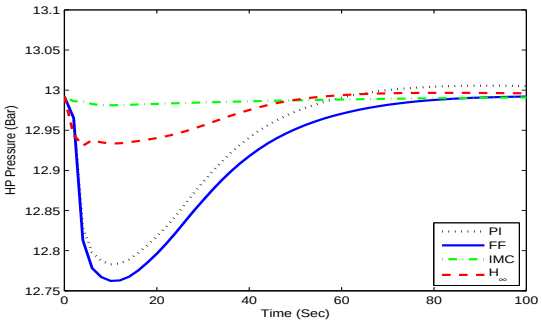

Fig. 9. HP regulation transient performance.

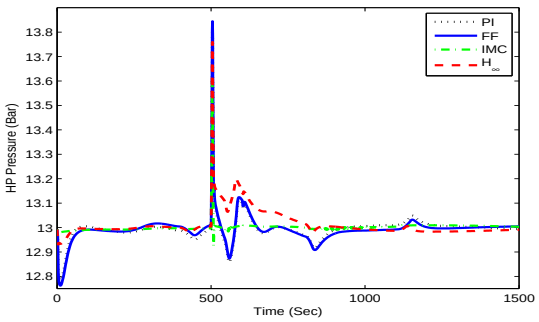

Fig. 10. HP regulation performance with a turbine trip.

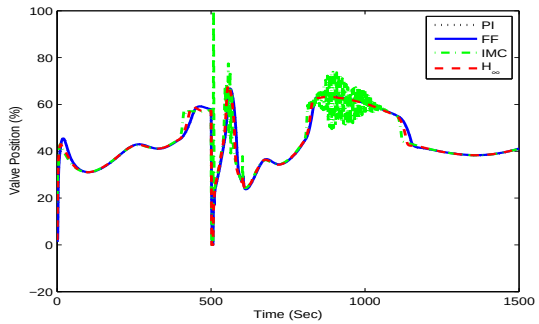

Fig. 11. Sliding valve position with a turbine trip.

Note that the possible algebraic loop issue (in case $E \neq 1$) can be resolved using the idea as in [15].

V. Simulation and Discussion

A. Simulation in EcosimPro

To verify the proposed control method, real-time simulation results in the software EcosimPro are given. Several cases are simulated:

- **Time-varying disturbance**: The simulation is first conducted with a time-varying heat load $d(t) = 80\sin(0.005t) + 200$ applied in the reservoir. Several control methods, PI control (PI), feedforward control (FF), internal model control (IMC) and the proposed H_∞ control, are tested. Comparative simulation results are provided in Fig.8 and Fig.9. It is shown that the IMC can achieve best steady-state performance (i.e. smallest regulation error) and transient performance (i.e. fastest convergence speed). It is reasonable since the plant model and its inverse model are all directly utilized in the control implementation. Among other approaches, the H_∞ control gives smaller transient overshoot as well as the steady-state regulation error. The PI control has similar transient to FF control but gives larger steady-state error.
- **Turbine trip**: To evaluate the compensation for the windup effect, simulations are also performed with a turbine trip between 550-650Sec as [8]. Comparative regulation results are depicted in Fig.10, for which the IMC controller allows disturbances rejection with a faster recovery speed. However, the IMC imposes aggressive control behavior, i.e. with valve stem position fluctuations, which is shown in Fig.11. On the other hand, the proposed H_∞ control with AW gives smaller overshoot and steady-state regulation error and smoother transient performance compared to FF and PI. For more details, the corresponding controller outputs are also given in Fig.12, which shows that the proposed H_∞ control with the AW compensation almost avoids the saturation issue, i.e. the control output is within [0,100].

B. Discussion

From above simulations, it can be seen that the PI, FF, IMC and the proposed H_∞ control with AW have their own characteristics:

PI control: It has a simple control structure for implementation, and no plant model is used. Although the disturbance rejection can be improved with high gains, the oscillated transient is obtained or even the stability may be lost in the worst case. Moreover, the integral windup will degrade the control performance in the presence of control constraints.

FF control: The disturbance model and the plant model inverse are superimposed in the feedback control as an extra compensation for the disturbance. Consequently, the improved steady-state regulation can be expected. The problem is that the disturbances are assumed to be precisely measurable, and the plant models are assumed to be exactly known. Moreover, the robustness to modeling uncertainties

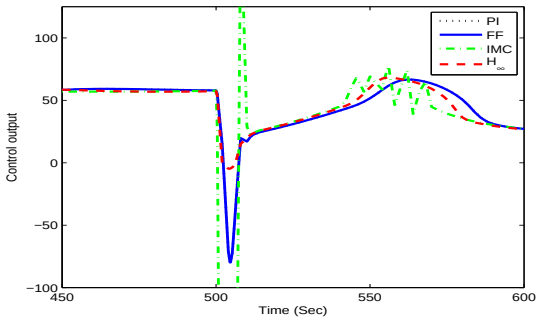

Fig. 12. Control output with a turbine trip.

are not considered.

IMC control: The plant model and its inverse are employed. Note in this paper the inverse model with a low pass filter is used as the feedback control, such that the disturbance rejection is guaranteed without any information on the disturbance measurement and its model. The robustness can be theoretically studied. Best output regulation performance has been achieved among the tested controllers. The complexity of the control design and implementation is moderate. However, the utilization of the model inverse as the feedback control action may introduce high gain and thus cause unexpected fluctuations and oscillation in the control actions (see Fig.11). This may be further remedied by redesigning the feedback control.

H_∞ control with AW: The modeling uncertainties can be explicitly considered in the H_∞ control synthesis, and 2-DOF feedback control also allows for the disturbance rejection with guaranteed robustness and performance. The valve control saturation is specifically compensated, which can further improve the transient performance when saturation occurs. However, a control with relatively high order may be derived following this synthesis, and the subsequent order reduction is necessary in the practical applications.

VI. Conclusions

System identification and advanced robust control is studied for a helium liquifier to regulate the discharge pressure of compressor station. Time-varying heat loads are applied in the reservoir to simulate dynamic responses. An anti-windup framework is adopted to compensate for the control valve saturation.

Comparative simulations conducted in the software EcosimPro reveal that the proposed robust AW control scheme works well in the presence of control valve saturation. It gives designers more freedom to tradeoff the robustness and performance (i.e. the modeling uncertainties and disturbance rejection are explicitly considered in the control synthesis). However, the control order reduction needs to be studied before applying this control scheme to actual system. On the other hand, among the tested controllers (PI, FF, IMC and H_∞), IMC can achieve good regulation and disturbance rejection performance in terms of transient and steady-state. Nevertheless, the possible high gain control due to the model inverse may trigger the valve saturation and thus result in aggressive control actions, which may be overcome by redesigning the feedback control part. Moreover, the frequency-domain identification approach provides fairly precise models that cover system dynamics among a wide frequency band.

Acknowledgment

The authors would like to thank Dr. Benjamin Bradu and Mr. William Booth in CERN for sharing the cryogenic models and also for their support in the collaborative work. The authors also appreciate all staffs in the ITER cryogenic system section for their supports.

Disclaimer

References

[1] R. Aymar, P. Barabaschi, and Y. Shimomura. The ITER design. *Plasma physics and controlled fusion*, 44:519–565, 2002.

[2] L. Serio et al. Challenges for cryogenics at ITER. In *AIP Conference Proceedings*, volume 1218, pages 651–633, 2010.

[3] V. Kalinin, E. Tada, F. Millet, and N. Shatil. ITER cryogenic system. *Fusion engineering and Design*, 81(23-24):2589–2595, 2006.

[4] M. Kalinin V. Henry D. Sanmarti M. Serio, L. Chalifour and B. Sarkar. conceptual design of the cryogenic system for ITER. In *Proceedings of the 22nd International Cryogenic Engineering Conference*, 2008.

[5] R. Maekawa, K. Ooba, M. Nobutoki, and T. Mito. Dynamic simulation of the helium refrigerator/liquefier for LHD. *Cryogenics*, 45(3):199–211, 2005.

[6] B. Bradu, P. Gayet, and S.I. Niculescu. A process and control simulator for large scale cryogenic plants. *Control Engineering Practice*, 17(12):1388–1397, 2009.

[7] B. Bradu, P. Gayet, and S.I. Niculescu. Modeling, simulation and control of large scale cryogenic systems. In *Proceedings of the 17th IFAC World Congress*, pages 13265–13270, 2008.

[8] B. Bradu, P. Gayet, and S.I. Niculescu. Control optimization of a LHC 18 kw cryoplant warm compression station using dynamic simulations. In *AIP Conference Proceedings*, volume 1218, pages 1619–1627, 2010.

[9] E. Blanco, C. de Prada, S. Cristea, and J. Casas. Nonlinear predictive control in the LHC accelerator. *Control Engineering Practice*, 17(10):1136–1147, 2009.

[10] R. Maekawa, S. Takami, and M. Nobutoki. Adaptation of advanced control to the helium liquefier with C-PREST. In *Proceedings of the 22nd International Cryogenic Engineering Conference*, pages 243–248, 2008.

[11] F. Clavel, M. Alamir, P. Bonnay, A. Barraud, G. Bornard, and C. Deschildre. Multivariable control architecture for a cryogenic test facility under high pulsed loads: Model derivation, control design and experimental validation. *Journal of Process Control*, 21(7):1030–1039, 2011.

[12] B. Bradu. Tutorial: Modeling of cryogenic systems with Ecosimpro. Technical report, CERN. Geneva, Switzerland, 2011.

[13] K. Zhou, J. C. Doyle, and K. Glover. *Robust and optimal control*. Prentice Hall, Upper Saddle River, N.J., 1996.

[14] S. Skogestad and I. Postlethwaite. *Multivariable feedback control analysis and design*. John & Sons, Ltd, 2005.

[15] G. Li, G. Herrmann, D. P. Stoten, J. Tu, and M. C. Turner. A novel robust disturbance rejection anti-windup framework. *International Journal of Control*, 84(1):123–137, 2011.

[16] EA Internacional. Ecosimpro 4.4: Mathematical algorithms and simulation guide. Technical report, Madrid, Spain., 2007.

[17] Cryodata Inc. Users guide to HEPAK version 3.4. Technical report, Cryodata Inc, Louisville, Colorado, USA, 1999.

[18] L. Lennart. *System identification: theory for the user*. PTR Prentice Hall, Upper Saddle River, NJ, 1999.

[19] A. Zheng, V.K. Mayuresh, and M. Morari. Anti-windup design for internal model control. *International Journal of Control*, 60(5):1015–1024, 1994.

[20] P. F. Weston and I. Postlethwaite. Linear conditioning for systems containing saturating actuators. *Automatica*, 36:1347–1354, 2000.

[21] G. Li, G. Herrmann, D. P. Stoten, J. Tu, and M. C. Turner. Application of robust antiwindup techniques to dynamically substructured systems. *IEEE/ASME Transactions on Mechatronics*, Accept for publication, 2011.